Magnetic Structure of Manganese Chromite*

J. M. HASTINGS AND L. M. CORLISS
Chemistry Department, Brookhaven National Laboratory, Upton, New York
(Received December 1, 1961)

An investigation of the magnetic structure and properties of $MnCr_2O_4$ has been carried out by means of neutron diffraction and an evaluation of the suitability of various proposed theoretical models has been made. From room-temperature diffraction patterns it is established that $MnCr_2O_4$ is a normal spinel with a u parameter of 0.3892 ± 0.0005 and with less than one percent of the Mn^{++} ions present on B sites. The Curie temperature, as determined from diffraction data, is $\sim$43°K. Below this temperature the magnetic contribution to the fundamental spinel peaks arising from aligned spins increases as the temperature is lowered and is effectively saturated at about 20°K. At 18°K, additional sharp peaks appear at positions which cannot be indexed either on the original unit cell or on any reasonably enlarged cell. These extra reflections persist with unchanged intensities down to 4.2°K. No change in either the positions or intensities of the fundamental lines is observed in going through the transition. Above 18°K, a diffuse peak is present in the region where the principal extra lines develop. This diffuse peak decreases with increasing temperature, but is still observable above the Curie point. Application of a magnetic field along the neutron scattering vector decreases the magnetic contributions to the fundamentals, but increases the intensities of the extra reflections.

The Néel model and the Yafet-Kittel model fail to account for major qualitative features of the diffraction results. On the other hand, the ferrimagnetic spiral model of Lyons, Kaplan, Dwight, and Menyuk is in good qualitative accord with all the observations. A detailed comparison with the theoretical predictions is presented and attention is called to broad areas of agreement as well as to certain discrepancies. The general conclusion reached is that the spiral model is a good first approximation to the ground-state spin configuration.

INTRODUCTION

THE first systematic investigation of the magnetic properties of chromites by McGuire, Howard, and Smart[1] revealed a number of puzzling features which could not be explained in terms of the Néel[2] theory. Later studies, particularly of mixed ferrite-chromite systems produced further evidence of anomalous behavior associated with the presence of a high concentration of Cr^{3+} ions on octahedral sites.

McGuire *et al.*[1,3] measured the saturation magnetization and the temperature dependence of the paramagnetic susceptibility of Mg, Mn, Co, Ni, Cu, and Zn chromites; the Fe compound was studied by Lotgering.[4] Mg and Zn exhibit normal paramagnetic behavior corresponding to a spin-only moment for Cr^{3+}. Susceptibilities of the remaining members of the series have the characteristic temperature dependence predicted by Néel for ferrimagnetic spinels, but whereas the effective moments for Mn and Fe have the spin-only value, those for Co, Ni, and Cu are appreciably higher. The saturation magnetizations for Fe, Co, Ni, and Cu are considerably lower than that given by the Néel model. On the other hand, the spontaneous moment for the Mn compound of[5] 1.2 μ_B is close to the theoretical spin-only value of 1.0 μ_B.

Numerous attempts have been made to bridge the gap between the ferrites, which are well behaved in terms of the Néel theory, and the chromites, which are anomalous, by the study of chromite-ferrite solid solutions, $MFe_{2-t}Cr_tO_4$, where t ranges from 0 to 2. Gorter[6] has considered the experimental findings on chromites as well as his own results on the Li chromite-ferrite and the Mn chromite-ferrite systems and has attempted to explain the results on the basis of non-collinear spins as suggested by the Yafet-Kittel[7] modification of the Néel theory. He postulates that angles are present between B-site moments both in pure $MnCr_2O_4$ and in the chromium-rich solid solutions with Li ferrite and Mn ferrite.

Lotgering[4] has given a detailed analysis of the case of a normal spinel from the point of view of the Yafet-Kittel theory. He shows that magnetic properties of both $MnCr_2O_4$ and $FeCr_2O_4$ are consistent with a triangular arrangement of moments in which angles occur on B sites. A similar analysis was carried through by Edwards[8] for the system Mn chromite-aluminate, where it is found that the magnetic properties can be qualitatively explained by the presence of angles between chromium moments on B sites.

Additional studies of ferrite-chromite solid solutions[9] have indicated anomalous saturation moments for Cr-rich solid solutions, suggesting in some instances, non-parallelism of the B-site moments. McGuire and Greenwald[9] have also investigated several chromite-ferrite solid solutions in which further substitutions of Zn^{++}, Al^{3+}, and Ga^{3+} were made. The behavior of the saturation moment as the Cr-Fe ratio is varied is explained by these authors by assuming that an appropriate fraction

* Research performed under the auspices of the U. S. Atomic Energy Commission.

[1] T. R. McGuire, L. N. Howard, and J. S. Smart, Ceram. Age **60**, 22 (1952).

[2] L. Néel, Ann. phys. **3**, 167 (1948).

[3] W. G. Schindler, T. R. McGuire, L. N. Howard, and J. S. Smart, Phys. Rev. **86**, 599 (1952).

[4] F. K. Lotgering, Philips Research Repts. **11**, 190 (1956).

[5] The saturation moment was originally reported by McGuire *et al.*[1] as 1.5 μ_B, but was corrected as noted by P. L. Edwards [Bull. Am. Phys. Soc. **3**, 43 (1958)]. Later measurements by other investigators have given values ranging from 1.16 to 1.22.

[6] E. W. Gorter, Philips Research Repts. **9**, 295, 321, 403 (1954).

[7] Y. Yafet and C. Kittel, Phys. Rev. **87**, 290 (1952).

[8] P. L. Edwards, Phys. Rev. **116**, 294 (1959).

[9] S. Miyahara and H. Ohnishi, J. Phys. Soc. Japan **11**, 1296 (1956); S. Miyahara and T. Tsushima, *ibid.* **13**, 758 (1958); T. R. McGuire and S. W. Greenwald, *Proceedings of the International Conference on Solid State Physics, Brussels, 1958* (Academic Press Inc., New York, 1960), Vol. 3, p. 50.

of the B-site moment is reversed. Wickham and Goodenough[10] have also shown that generally good agreement between observed and calculated saturation moments can be obtained for a series of chromites and mixed ferrite-chromites if some of the Cr^{3+} moments are parallel, rather than antiparallel, to the A-site moments.

Several attempts have been made to detect the presence of Yafet-Kittel angles by means of neutron diffraction. The existence of angles between moments on face-centered substructures of either the A or B sites, as envisaged by the theory, should give rise to intensity at the normally forbidden (200) position as well as at the normal spinel line positions. Prince[11] has examined the magnetic contributions to the diffraction pattern of $CuCr_2O_4$ at 77°K and has concluded that the results can only be explained by the presence of nonparallel spins on B sites. While a unique solution is not obtained from the powder data, the observations are consistent with a configuration of the Yafet-Kittel type. Nathans, Pickart, and Miller,[12] in a more recent investigation, have confirmed these conclusions by studying the field dependence of the magnetic contributions to the diffraction pattern. They find that the Cr^{3+} moments are nearly antiparallel to each other and approximately perpendicular to the net magnetization. Pickart and Nathans[13] have also looked for evidence of triangular spin arrangements in the $MnFe_{2-t}Cr_tO_4$ and $NiFe_{2-t}Cr_tO_4$ systems. No ordering such as would be expected for the Yafet-Kittel model was observed at the compositions investigated, but it was found that in those cases where the Néel model failed, the magnetic scattering was consistent with antiparallel A- and B-site magnetizations and a reduced moment on B sites. Baltzer and Wojtowicz[14] have proposed that the low B-site moments observed in chromites by neutron diffraction and by magnetic measurements result from the production of a low-spin state of the Cr^{3+} ion under the influence of the Jahn-Teller distortion of neighboring ions.

Jacobs[15] has measured the magnetization of a number of spinels at high pulsed fields and at low temperatures and has used the differential susceptibility as a criterion for detecting noncollinear spin arrangements. He has interpreted the results for a number of ferrites, chromites, and mixed ferrite-chromites to indicate the presence of triangular ferrimagnetic arrangements. For the case of $MnCr_2O_4$ in particular, the measurements support a configuration of the Yafet-Kittel type; however, as the author points out, they are not inconsistent with more general models in which individual moments are inclined to the direction of net magnetization.

Lyons and Kaplan[16] have recently developed a generalization of the Luttinger and Tisza method for finding the classical ground state of a lattice with Heisenberg exchange interactions and have applied the results to spinels in which both A-B and B-B nearest-neighbor interactions are important. In the case of a cubic spinel, they show that appreciably lower energy than that given by the Yafet-Kittel model can be achieved by a ferrimagnetic spiral. According to this model, spins belonging to a given sublattice have directions lying on the surface of a cone whose half-angle is fixed. The axial components of spins on one sublattice are constant, but the transverse components rotate in discrete steps under translation to equivalent sites in other unit cells along a fixed direction in the crystal (propagation direction). In the general case, each sublattice is characterized by a cone angle and a phase angle for the rotation of the transverse component. The axes of the cones corresponding to different sublattices are parallel but need not coincide with the direction of propagation of the spiral. Over an appreciable range of the ratio of the B-B to the A-B interaction, the conical model is found to be locally stable with respect to small deviations in the individual spin components and to minimize the energy for a large class of possible spin configurations. Calculations by Lyons, Kaplan, Dwight, and Menyuk[17] (LKDM) for the case of a normal cubic spinel provide a detailed picture of the conical model appropriate to $MnCr_2O_4$. In the present paper the results of a neutron diffraction study of $MnCr_2O_4$ will be presented and compared with the various theoretical models of the magnetic structure and with modifications suggested by magnetic measurements on pure and mixed chromites.

EXPERIMENTAL

The specimen of $MnCr_2O_4$ used in the present investigation was provided through the courtesy of Dr. A. Wold of the Lincoln Laboratory. It was prepared[18] by a "precursor" technique in which crystalline $MnCr_2O_7 \cdot 4C_5H_5N$, containing the metallic species in the desired atomic ratio, was first ignited to give finely divided and intimately mixed oxides. The oxides were then fired at 1100°C in air to produce the chromite and quenched from about 800°C. This was followed by a final firing at 1100°C in a 1:3 hydrogen-nitrogen atmosphere to convert all the manganese to the divalent state. The final product was characterized[18] by a Cr^{3+}/Mn^{++} ratio of 2.015 ± 0.002, a lattice constant of 8.437 ± 0.002, and a saturation magnetic moment of $1.20\ \mu_B$, measured in a field of 10 000 oe at 4.2°K.

Neutron diffraction patterns were obtained at room temperature, and at the temperatures of liquid N_2, H_2,

[10] D. G. Wickham and J. B. Goodenough, Phys. Rev. **115**, 1156 (1959).
[11] E. Prince, Acta Cryst. **10**, 554 (1957).
[12] R. Nathans, S. J. Pickart, and A. Miller, Bull. Am. Phys. Soc. **6**, 54 (1961).
[13] S. J. Pickart and R. Nathans, Phys. Rev. **116**, 317 (1959).
[14] P. K. Baltzer and P. J. Wojtowicz, J. Appl. Phys. **30**, 27S (1959).
[15] I. S. Jacobs, J. Phys. Chem. Solids **15**, 54 (1960).
[16] D. H. Lyons and T. A. Kaplan, Phys. Rev. **120**, 1580 (1960).
[17] D. H. Lyons, T. A. Kaplan, K. Dwight, and N. Menyuk, preceding paper [Phys. Rev. **126**, 540 (1962)].
[18] E. Whipple and A. Wold, Massachusetts Institute of Technology Lincoln Laboratory Group Report, 53-G-0060, 1961 (unpublished); J. Phys. Chem. Solids (to be published).

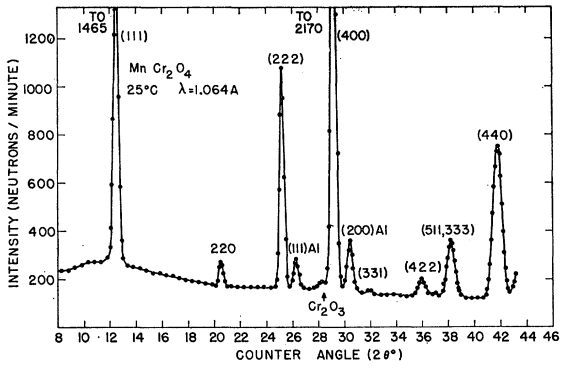

FIG. 1. Room temperature diffraction pattern of polycrystalline $MnCr_2O_4$. The reflections labeled Al are produced by the aluminum specimen holder.

and He. In addition, a number of slow-warming curves were run in order to locate magnetic transitions, and at the lowest temperature, the effect of magnetization on the magnetic scattering was studied in an applied field of about 10 000 oe. The wavelength employed in the diffraction experiments was 1.064 Å throughout.

DETERMINATION OF STRUCTURAL PARAMETERS

It has been assumed by many investigators that the chromites have the normal spinel structure. The preference of the Cr^{3+} ion for B sites is strongly suggested by the work of Verwey and Heilmann[19] in which the lattice constants of the aluminates, chromites, and ferrites are intercompared and correlated with experimentally-determined ionic distributions for several members of each series. Prince[11,20] has shown by means of neutron diffraction that $CuCr_2O_4$ and $NiCr_2O_4$ are normal spinels. Edwards,[8] using the x-ray method of Bertaut[21]

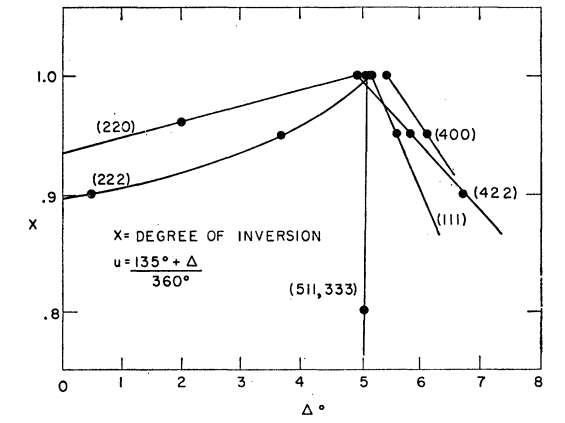

FIG. 2. Dependence of the degree of inversion upon the u parameter for various reflections. The intersection represents values of x and u which simultaneously fit the intensities of all observed nuclear peaks.

together with a semi-empirical value for the oxygen parameter, has concluded that $MnCr_2O_4$ is essentially normal. Indirect diffraction and magnetic evidence from studies of mixed systems[6,13,22] as well as theoretical studies[23,24] reinforce the conclusion that Cr^{3+} ions prefer surroundings of octahedral symmetry.

The cation distribution and the oxygen parameter have been determined for $MnCr_2O_4$ from room temperature data (Fig. 1) using a graphical method. Calculated intensities for a given reflection were plotted as a function of the oxygen parameter u, for different values of the degree of inversion x, defined by the expression $Mn_xCr_{1-x}[Mn_{1-x}Cr_{1+x}]O_4$, where the brackets refer to B sites. The suitably normalized observed intensity, drawn as a horizontal line on such a plot, intersects the calculated curves in points representing compatible values of x and u. The allowed values of x have been replotted as a function of u in Fig. 2 for a number of reflections. It is readily seen that the curves in Fig. 2 have a common intersection which determines a unique set of parameters for which all reflections are simultaneously satisfied. In this way one obtains values of $u=0.3892\pm0.0005$ and $x=1.00\pm0.01$, indicating that $MnCr_2O_4$ is indeed a normal spinel. A comparison of observed intensities with those calculated using the above values for the structural parameters is given in Table I.

TABLE I. Comparison of calculated and observed integrated intensities (nuclear)—300°K.

hkl	Calculated[a]	Observed
111	18 190	18 760
220	1080	1100
311	18	0
222	12 540	12 570
400	32 740	33 560
331	180	150
422	1630	1580
511, 333	6080	6110
440	18 060 ⟷	18 060

[a] Completely regular spinel, $u=0.3892$.

MAGNETIC SCATTERING

The diffraction pattern remains unchanged as the temperature is lowered to 77°K, except for a slight temperature effect on the coherent scattering and for certain changes in the background which will be described later. Below the Curie point the intensities of a number of the fundamental spinel peaks increase abruptly as a result of the superposition of magnetic contributions arising from aligned spins. The temperature dependence of this magnetic component was studied by following the peak intensity of the (111)

[19] E. J. W. Verwey and E. L. Heilmann, J. Chem. Phys. **15**, 174 (1947).
[20] E. Prince, J. Appl. Phys. **32**, 68S (1961).
[21] E. F. Bertaut, J. phys. radium **12**, 252 (1951).
[22] F. C. Romeijn, Philips Research Repts. **8**, 304, 321 (1953).
[23] J. H. van Santen and J. S. van Wieringen, Rec. trav. chim. **71**, 420 (1952).
[24] J. B. Goodenough and A. L. Loeb, Phys. Rev. **98**, 391 (1955).

reflection as the sample was allowed to warm slowly from helium temperatures. The results, shown in Fig. 3, indicate a Curie point of about 43°K, in good agreement with the value of 41°K obtained by Menyuk *et al.*,[25] from magnetic measurements, but appreciably lower than the earlier estimate of 55°K reported by McGuire and Greenwald.[9] The ordinate in Fig. 3 is the magnetic structure factor for the (111) reflection and is roughly proportional to the average of the A- and B-site moments. (For the Néel model the structure factor is proportional to the quantity $|\mu_A|+\sqrt{2}|\mu_B|$; however, somewhat more complicated expressions are required for noncollinear models.) Indirect evidence that the Curie point cannot be very much higher than 43°K was obtained by studying the (111) reflection at temperatures of pumped nitrogen; no variation in intensity was detected down to 46°K.

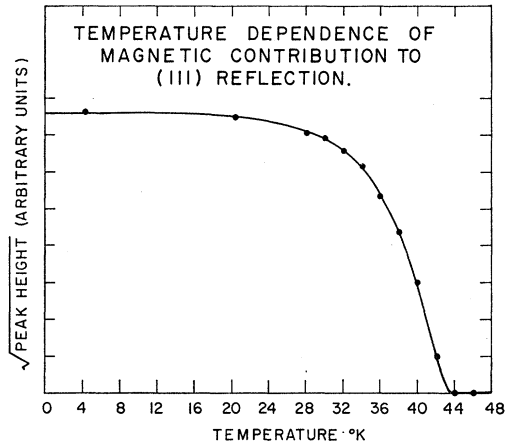

FIG. 3. Temperature dependence of the magnetic contribution to the (111) reflection.

As indicated in Fig. 3, the magnetic contribution to the fundamental spinel reflections is essentially saturated at about 20°K. Diffraction patterns obtained at the fixed points 20.4° and 4.2°K (Fig. 4) are indeed identical with respect to the fundamental peaks. At 18°K, however, an ordering transition occurs, as evidenced by the appearance of additional sharp lines in the diffraction pattern. The extra reflections arise at nonsimple positions in the pattern and cannot be indexed either on the original unit cell or on any reasonably enlarged cell. Above 18°K, a broad diffuse peak is present in the region where the principal extra line develops and may represent a state of short-range magnetic order. The growth of the diffuse peak, as the temperature is lowered from room temperature, is shown in Fig. 5. The actual transition at 18°K is quite sharp; its temperature dependence was obtained by following the variation of the peak height of the principal extra line as the sample warmed slowly from

[25] N. Menyuk, A. Wold, D. Rogers, and K. Dwight (to be published).

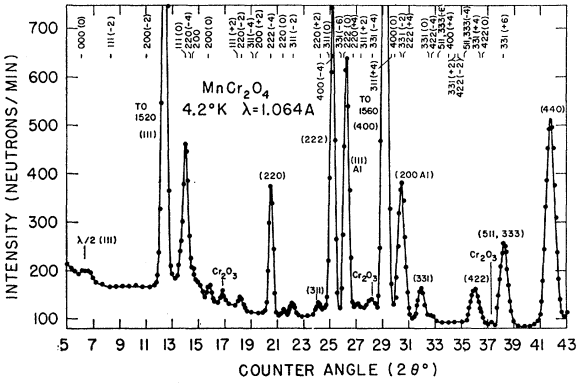

FIG. 4. Liquid helium temperature diffraction pattern of $MnCr_2O_4$. The indices at the top of the figure represent all the possible satellite reflections over the angular interval plotted.

4.2°K through the transition (Fig. 6). The constancy of the peak height between 4.2° and about 15°K suggests, but does not completely establish, that no further transition occurs in this temperature range.

In an ordinary ferromagnetic or ferrimagnetic material, in which spins are all parallel or antiparallel to a fixed direction in a given magnetic domain, the contribution of the aligned moments to the diffraction peaks can be determined by application of a magnetic field sufficient to saturate the magnetization in a suitable direction. If the field is directed parallel to the scattering vector, i.e., along the normal to a set of crystallographic planes for which the diffracted intensity is being re-

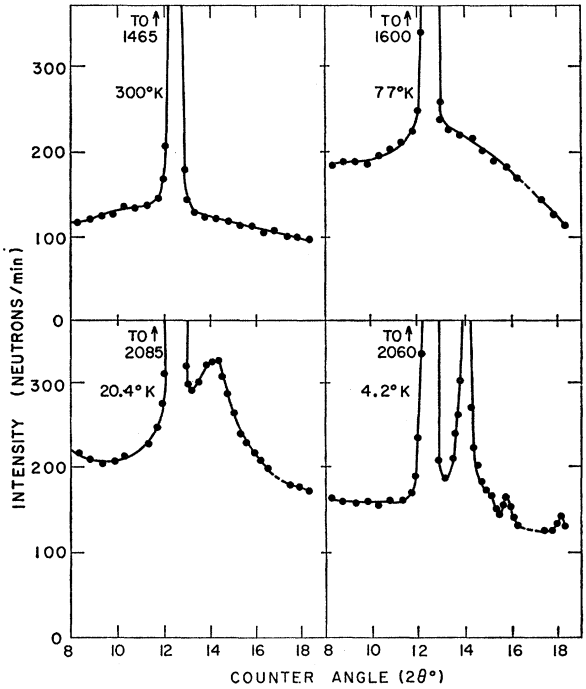

FIG. 5. Temperature dependence of the background in the neighborhood of the (111) reflection, showing the gradual development of long-range order.

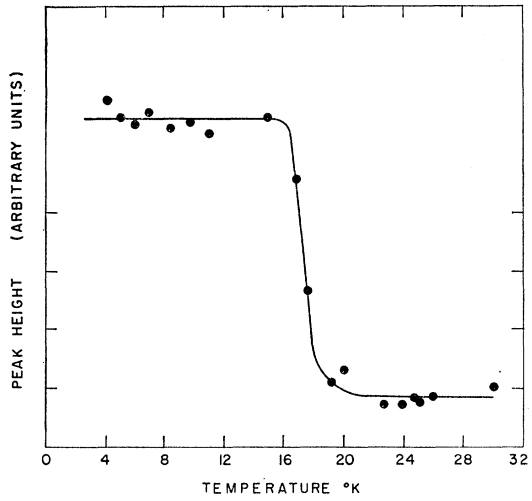

FIG. 6. Temperature dependence of the peak height of the principal extra reflection, 111 (0).

corded, the magnetic contribution disappears. For non-collinear spin arrangements, the component parallel to the field would be "quenched" whereas the contributions arising from perpendicular components would be enhanced. Diffraction patterns obtained for $MnCr_2O_4$ at 4.2°K both in zero field and in a field of approximately 10 000 oe, exhibit precisely this type of behavior. With the field oriented parallel to the scattering vector, the magnetic contributions to the (111) and (220) peaks are reduced to zero, whereas the intensity of the principal extra reflection is *increased* by about fifty percent, which is the amount to be expected in going from the unmagnetized state, with a random distribution of domains, to the saturated condition. These results indicate that the magnetic contributions to the fundamentals arise from components of the spins parallel to the net magnetization and that the extra lines are produced by the perpendicular components.

CONSIDERATION OF POSSIBLE MODELS

The various models to be considered in relation to the experimental findings on $MnCr_2O_4$ can be classified as follows: (a) the Néel model with spin-only values for both the Mn^{++} and Cr^{3+} moments, (b) the Néel model with Cr^{3+} ions in low-spin states, (c) a modified Néel model in which some reversed spins are present on A and B sites, (d) the Yafet-Kittel triangular model, with angles on either A or B sites, and (e) the ferrimagnetic spiral or conical model.

The salient feature of the diffraction data between the Curie point and the transition at 18°K is that the magnetic contributions to the fundamental peaks are appreciably lower than would be expected for ions with spin-only moments ordered according to the Néel scheme. Intensities computed for this arrangement are given in the second column (model 1) of Table II. The observed magnetic intensities listed in the table were obtained by subtracting the calculated nuclear contributions from the diffraction pattern at 4.2°K. (The same result is obtained by subtracting the 77°K pattern from that at helium temperature and correcting for the effect of temperature on the coherent intensities.) By far the most important criterion for judging the extent of agreement between calculated and observed intensities is the fit obtained for the (111) and (220) reflections. The (311) intensity is too weak for reliable comparison and the (222) and (400) magnetic components, while appreciable, are largely masked by the nuclear scattering. A five percent change in the total intensity of the last two reflections results in a fifty percent change in the magnetic part. The (331) and (422) reflections are once again quite reliable but agreement to within ten to twenty percent is all that can be expected because of imperfect knowledge of the magnetic form factor and the temperature factor at higher angles.

While the Néel model, taken together with spin-only moments, gives calculated magnetic intensities which are three to four times too high, it is possible to obtain a satisfactory empirical fit using an A-site moment of 3.56 μ_B and a B-site moment of 1.50 μ_B, as indicated for model 2 in Table II. Unfortunately, this device results in a macroscopic net moment of 0.56 μ_B per molecule, which is about one-half the observed value. The introduction of reversed spins on A and B sites could indeed account for the low empirical moments but would not explain the macroscopic moment. Spin quenching of the Cr^{3+} moments would achieve even less since it does not provide for the reduction of the A-site moment. The Yafet-Kittel model can explain the reduction of either the A-site moment or the B-site moment but not both simultaneously. The conical model, on the other hand, does provide a mechanism for reducing the scattering power on both sites and can be made to fit the macroscopic moment.

These conclusions are reinforced by considering the effect of a magnetic field on the intensities of the extra lines which appear below 18°K. All models based on the

TABLE II. Comparison of calculated and observed integrated intensities (magnetic)—4.2°K.

	Calculated			
hkl	Model 1[a]	Model 2[b]	Model 3[c]	Observed
111	49 130	12 410	12 000	12 000
220	10 910	3710	3710	3710
311	150	350	700	340
222	5210	870	590	870
400	7350	1740	1820	3100
331	7150	1810	1670	2130
422	2300	780	840	1000
511, 333	25	60	90	<100
440	0	0	0	0

[a] Néel Model $\mu(Mn) = 5\ \mu_B$, $\mu(Cr) = 3\ \mu_B$, $\mu(\text{molecule}) = 1\ \mu_B$.
[b] Néel Model $\mu(Mn) = 3.56\ \mu_B$, $\mu(Cr) = 1.50\ \mu_B$, $\mu(\text{molecule}) = 0.58\ \mu_B$.
[c] Spiral Model $\mu(Mn) = 3.68\ \mu_B$, $\mu(Cr_1) = 1.46\mu_B$, $\mu(Cr_2) = 1.01\ \mu_B$ $\mu(\text{molecule}) = 1.21\ \mu_B$

Néel scheme, including the reversed spin and spin-quenched modifications, predict a decrease in intensity on application of a field, whereas the reverse is found experimentally. The experimental result points, in fact, to an ordered noncollinear structure in which the components of the spins perpendicular to the net moment give rise to the extra lines.

The suitability of a conical or ferrimagnetic spiral model is made all the more plausible by a consideration of the positions of the extra lines in the diffraction pattern. A spiral modulation of the spin structure gives rise to a splitting of each spot in reciprocal space into components, or satellites, which are arranged symmetrically about the original position and displaced parallel to the propagation direction. The observed d spacings will then be given by the reciprocals of the distances from the origin of reciprocal space to the satellite spots and will not necessarily exhibit any simple relationship to the chemical cell dimensions. It is in principle possible, by choosing a sufficiently large unit cell, to index the reflections in almost any powder pattern. (In the present instance, the observed lines can be indexed on a cell having 27 times the volume of the spinel unit cell, or 432 chromium atoms.) The difficulty arises in accounting for the absence of the large number of reflections which are geometrically possible in such a cell. Although a conical spin structure will in general correspond to a very large unit cell, the model provides a simple physical mechanism to account for the relatively small number of observed reflections.

The Yafet-Kittel model, on the other hand, predicts extra intensity in the low-angle region only at the (200) position, and thus fails to account even qualitatively for the low-temperature pattern. It is conceivable, however, that a modification of the model in which angles are present on both A and B sites could explain the observations, provided the canted substructures were ordered in some scheme having a repeat distance at least three times that of the original spinel cell.

THE CONICAL MODEL

The problem of determining the ground-state spin configuration of spinels has been the subject of several theoretical discussions. When the only nonzero interactions are those between A-site and B-site spins, the Néel model is rigorously the ground state. However, when competing interactions, in particular B-B interactions, can no longer be neglected, the problem becomes a complex one. Lyons and Kaplan[16] have succeeded in proving that the Néel model remains the ground state over the range $u \leqslant u_0 = 8/9$, where

$$u = (4J_{BB}S_B)/(3J_{AB}S_A).$$

This proof is based on an extension of the Luttinger-Tisza method for determining the minimum of a quadratic form subject to certain constraints. The energy of the system is assumed to be given by a classical Heisenberg exchange model. In an accompanying paper by LKDM,[17] further application is made of the generalized Luttinger-Tisza method in order to determine the true ground state for $u > u_0$. (As had already been shown,[26] the Yafet-Kittel triangular configuration is never the ground state for cubic spinels.) In this paper the authors show that a magnetic spiral structure, i.e., a structure in which the spin lies on a cone and the radial component rotates with a fixed wavelength in a given direction, has appreciably lower energy than the Yafet-Kittel configuration. They show that this ferrimagnetic spiral is the best of a large class of configurations and that it is locally stable with respect to small deviations of all the spin vectors if $u < 1.298$.

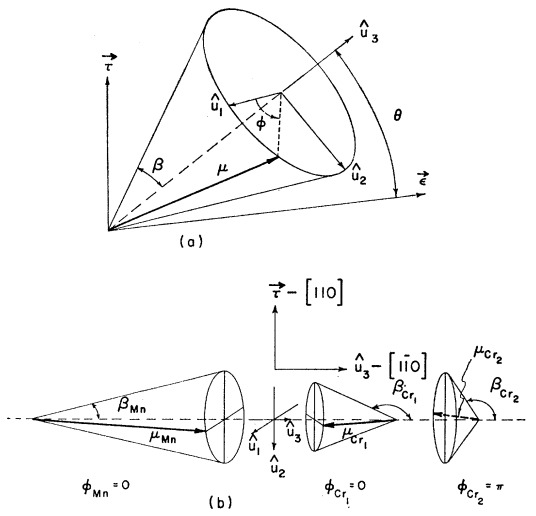

FIG. 7. (a) Coordinate system for spin vector $\mathfrak{u}$ lying on a cone of half-angle β. $\boldsymbol{\tau}$ is the propagation vector for the spin system and $\boldsymbol{\varepsilon}$ is the scattering vector for a given reflection. (b) Relative orientation of spins on the three substructures of $MnCr_2O_4$. The phase angles are indicated below the respective cones.

In the ferrimagnetic spiral structure the νth spin in the nth unit cell, $\mathbf{S}_{n\nu}$, is given by

$$\mathbf{S}_{n\nu} = |S_\nu| \sin\beta_\nu \left[\frac{\hat{u}_1 - i\hat{u}_2}{2} \exp[2\pi i \boldsymbol{\tau}\cdot\mathbf{r}_{n\nu}] e^{i\phi_\nu} + \text{complex conjugate} \right] + \hat{u}_3 |S_\nu| \cos\beta_\nu,$$

where $\hat{u}_1$, $\hat{u}_2$, and $\hat{u}_3$ are unit vectors of an orthogonal coordinate system attached to the cone on which the spin lies ($\hat{u}_3$ coincides with the cone axis). The half-angle of the cone is β, $\boldsymbol{\tau}$ is the propagation vector for the transverse or rotating component of the spin, ϕ_ν is the phase angle of the νth spin in the unit cell, and $\mathbf{r}_{n\nu}$ is the position vector. Figure 7(a) gives a schematic representation of this cone structure. The model proposed by LKDM leads to a decomposition of the spinel structure into three substructures, one composed of the tetra-

[26] T. A. Kaplan, Phys. Rev. **119**, 1460 (1960).

hedral sites and the other two of the octahedral sites. This subdivision of the octahedral sites into substructures is identical with the one postulated by Verwey, Haayman, and Romeijn[27] for the low temperature form of Fe_3O_4. The overall structure can be considered as made up of A-site cones with a given half-angle antiparallel to two different B-site cones each with its own half-angle; all three sets of transverse components being associated with a single propagation vector. There is a fixed phase relationship between the spins on the A and B substructures. This is shown schematically in Fig. 7(b).

The diffracted intensity is determined by $|F|^2$, which, for a general cone structure is given by

$$\begin{aligned} |F|^2 &= N^2(\sin^2\theta)A^2, \qquad \text{(fundamentals)} \\ &= N^2\left(\frac{1+\cos^2\theta}{4}\right)T^2, \quad \text{(satellites)} \end{aligned} \tag{1}$$

where

$$A=\sum_\nu \mu_\nu \cos\beta_\nu \exp(2\pi i \mathbf{B}_H\cdot\mathbf{r}_\nu),$$

and

$$T=\sum_\nu \mu_\nu \sin\beta_\nu e^{i\phi_\nu} \exp(2\pi i \mathbf{B}_H\cdot\mathbf{r}_\nu).$$

The axial components of the spin vectors give rise to the A term and contribute additional magnetic intensity only to the nuclear or fundamental peaks. This term may be considered as the usual Néel part of the conical model. In the expression for A, μ_ν is the moment of the νth magnetic species and $\mathbf{B}_H$ is a reciprocal lattice vector associated with the nuclear structure. The T term arises from the rotating component and is the structure factor for the satellite reflections, whose positions in reciprocal space are given by $\mathbf{B}_H\pm\boldsymbol{\tau}$. θ is the angle between the cone axis ($\hat{u}_3$) and the scattering vector (Fig. 7a). The coefficient of A^2 in Eq. (1) is the familiar q^2 factor for scattering from uniaxial spin structures; the T^2 term contains the analogous factor for a spiral. N is the total number of unit cells in the scatterer. A derivation of the intensity formulas for the ferrimagnetic spiral, as well as for more general spin configurations, is presented in the accompanying paper by LKDM. The case of a simple spiral has also been treated by Koehler,[28] using a different formalism.

It is seen from the expression for $|F|^2$ that the propagation vector, cone angles, cone-axis orientation, and relative phases, as well as the magnitudes of the spin vectors must be specified in order to fix both the angular position and intensity of the satellite and fundamental magnetic peaks. The theory of LKDM gives the propagation vector, cone angle, and relative phases as a function of the parameter u, which can be fixed by matching the observed saturation magnetization, assuming spin-only values for the moments of Mn^{++} and Cr^{3+}. The only quantity left unspecified by the theory is the orientation of the cone axis with respect to the crystal axes. It is the only adjustable parameter and must be determined by a comparison of calculated and observed intensities.

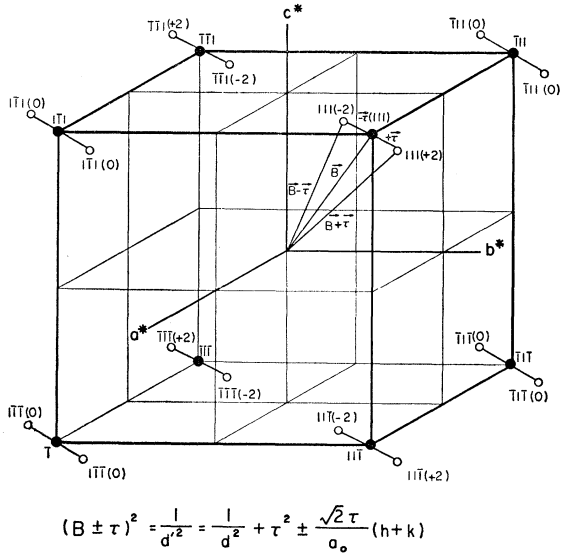

FIG. 8. Reciprocal lattice of $MnCr_2O_4$. The filled circles represent the eight (111) reciprocal lattice points and the open circles are the satellite points produced by a propagation vector along the [110] direction.

It has already been pointed out that the additional peaks which appear in the low temperature pattern cannot be indexed by any reasonable enlargement of the chemical unit cell. The conical model, on the other hand, provides a simple scheme for indexing peaks which appear to have nonintegral Miller indices. The satellite spots are associated with reciprocal-lattice vectors $\mathbf{B}_{H'}=\mathbf{B}_H\pm\boldsymbol{\tau}$; the corresponding interplanar spacing, $d_{H'}$, is given by

$$\frac{1}{d_{H'}{}^2}=(\mathbf{B}_H\pm\boldsymbol{\tau})^2=\frac{1}{d_H{}^2}+\tau^2\pm\frac{2|\boldsymbol{\tau}|}{a_0}(hu+kv+lw), \tag{2}$$

where h, k, l are the Miller indices of $\mathbf{B}_H$, a_0 the unit cell edge, and u, v, w the direction cosines of $\boldsymbol{\tau}$. Thus a given reflection is split into a number of peaks depending on the choice of propagation vector. Figure 8 is a diagram of the reciprocal lattice for $MnCr_2O_4$ in which the (111) points are explicitly exhibited. The direction of the propagation vector has been chosen, in accordance with LKDM, as [110] in this diagram and the splitting of the eight (111) reflections is shown. It can be seen that this choice of direction for $\boldsymbol{\tau}$ leads to three different values of $d_{H'}$. This can also be obtained from Eq. (2), which for $\boldsymbol{\tau}$ along [110], reduces to

$$\frac{1}{d_{H'}{}^2}=\frac{1}{d_H{}^2}+\tau^2\pm\frac{\sqrt{2}|\boldsymbol{\tau}|}{a_0}(h+k)$$

[27] E. J. W. Verwey, P. W. Haayman, and F. C. Romeijn, J. Chem. Phys. **15**, 181 (1947).
[28] W. C. Koehler, Acta Cryst. **14**, 535 (1961).

The possible values of $(h+k)$ for the {111} crystallographic form are 0 and ± 2 which accounts for the three satellites. (The notation to be used throughout to identify satellites arising from a [110] propagation vector consists of specifying the Miller indices of the parent peak together with the value of $(h+k)$.) The theory of LKDM fixes the wavelength as well as direction of τ and the fit between calculated and observed peak positions is shown graphically in Fig. 9. In this diagram $1/d_H'^2$ for satellites arising from the first few fundamental reflections is plotted against the wavelength of τ. On the vertical line drawn at $\tau=0.98$, which is the theoretically predicted wavelength, the observed $1/d'^2$ values of the satellites are indicated as horizontal markers. The thickness of these markers is equivalent to the uncertainty in the experimental peak positions. It is seen that the agreement between predicted and observed peak positions is good. In the interval plotted in the figure two relatively small peaks which cannot be indexed by this model have been omitted. At the present time there is no satisfactory explanation for these lines. There are a large number of intersections indicated on the diagram for which there are no observed satellites, but these are accounted for by the proposed model which predicts either zero or negligible intensity at these allowed positions.

The next step in the analysis, after indexing the satellites, is a comparison between calculated and observed integrated intensities. The model proposed by LKDM fixes the individual cone half-angles β_ν, and phase angles ϕ_ν, for the three substructures; but does not specify the angle ϑ, between the cone axis $\hat{u}_3$ and the scattering vector. Extensive calculations of integrated intensities have been made using the theoretical values of β_ν and ϕ_ν for various choices of cone axis. Attempts were made to vary β_ν and ϕ_ν about the predicted values, but even small variations lead to relatively large discrepancies in intensity. The results of these computations can be summarized by stating that the best agreement between calculated and observed integrated intensities of the satellite peaks is obtained for a model using the values of LKDM for β_ν and ϕ_ν and a cone axis along $[1\bar{1}0]$. The agreement realized in this way is semi-quantitative, but is surprisingly good considering the approximate validity of the model and the difficulty in obtaining accurate integrated intensities for small or unresolved satellite reflections. The comparison between calculated and observed intensities is given in Table III, where the following values have been used

$$\mu_\perp(\mathrm{Mn})=2.03\,\mu_B, \quad \beta(\mathrm{Mn})=23^\circ 56',$$
$$\mu_\perp(\mathrm{Cr_1})=1.39\,\mu_B, \quad \beta(\mathrm{Cr_1})=152^\circ 27',$$
$$\mu_\perp(\mathrm{Cr_2})=2.91\,\mu_B, \quad \beta(\mathrm{Cr_2})=103^\circ 53',$$
$$\phi(\mathrm{Mn})=0, \quad \mu(\mathrm{Mn})=5\,\mu_B,$$
$$\phi(\mathrm{Cr_1})=0. \quad \mu(\mathrm{Cr})=3\,\mu_B,$$
$$\phi(\mathrm{Cr_2})=\pi,$$

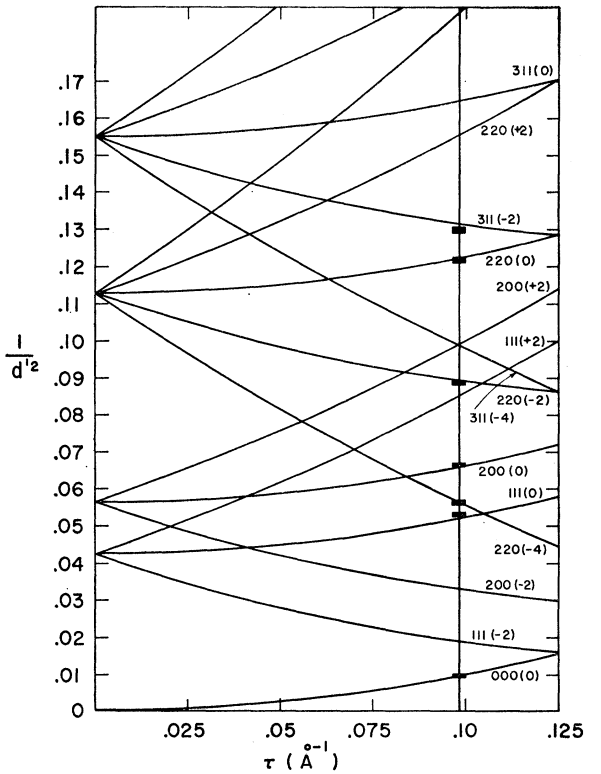

FIG. 9. Dependence of the splitting of the fundamentals on the wavelength of the [110] propagation vector. The vertical line at $\tau=0.983$ Å^{-1} is the theoretical value of LKDM. The horizontal markers are the experimental values of $1/d'^2$ for the observed satellites, where d' is the interplanar spacing. The thickness of these markers is a measure of the uncertainty in the observed peak positions.

and

$$\hat{u}_3 \| [1\bar{1}0].$$

The other experimental data which have to be accounted for are the magnetic contribution to the nuclear peaks, the fundamental magnetic reflections. The possibility of explaining these peaks in terms of a Néel model has already been mentioned, and the inconsistencies which arise, in particular with respect to the macroscopic moment, have been noted. The calculated fundamental magnetic intensities based on the theoretical model of LKDM are approximately 30% too high. In this case, however, it is possible to adjust the axial components of the spin vectors on the three substructures of the spiral model such that the observed macroscopic moment is fitted and at the same time satisfactory agreement is obtained between the calculated and observed intensities. This procedure results in the following axial components, $\mu(\mathrm{Mn})=3.68\,\mu_B$, $\mu(\mathrm{Cr_1})=-1.46\,\mu_B$, $\mu(\mathrm{Cr_2})=-1.01\,\mu_B$, giving a macroscopic moment of $1.2\,\mu_B$. The final intensity comparisons are given in Table II (model 3).

TABLE III. Comparison of calculated and observed integrated intensities (satellites)—4.2°K.

hkl	2θ	Calc.		Obs.		*hkl*	2θ	Calc.		Obs.	
000 (0)	6.10	95		150		222 (0)	26.02	120		Obscured	
111 (−2)	8.34	0		0		220 (+4)	26.80	290		Obscured	
200 (−2)	11.04	0		0		311 (+2)	27.42	440		Obscured	
?	13.6	...		790		331 (−4)	28.26	500		Obscured	
111 (0)	13.98	6300		7900		311 (+4)	29.70	50		Obscured	
220 (−4)	14.41	2100	8400	820	8700	400 (0)	29.92	120		Obscured	
[002]	14.50	30				331 (−2)	30.47	0		Obscured	
?	15.1	...		590		222 (+4)	30.60	20		Obscured	
200 (0)	15.74	1500		780		422 (−6)	30.68	80		Obscured	
111 (+2)	17.94	0		0		331 (0)	32.56	470	500	360	
220 (−2)	18.28	550		710		422 (−4)	32.75	30			
311 (−4)	19.16	250		0		333 (−6)	33.28	0		0	
200 (+2)	19.36	0		0		511 (−6)	33.28	0		0	
222 (−4)	20.50	90		Obscured		400 (+4)	34.02	90		0	
220 (0)	21.48	310		170		331 (+2)	34.52	0		0	
311 (−2)	22.23	1100		650		422 (−2)	34.72	70		0	
220 (+2)	24.28	210		Obscured		511 (−4)	35.20	30		0	
311 (0)	24.95	100		Obscured		331 (+4)	36.40	140		Obscured	
400 (−4)	25.21	400		Obscured		422 (0)	36.58	370		Obscured	
331 (−6)	25.86	0		Obscured		331 (+6)	38.20	0		Obscured	

DISCUSSION

The experimental situation may be summarized in the following way. The ferrimagnetic spiral model, which is expected to be only approximately valid for $MnCr_2O_4$, does indeed give a satisfactory qualitative account of the intensities of the satellite lines and explains the absence of nonobserved reflections. The theoretically determined parameters do, however, predict too much intensity for the fundamentals. On the other hand, empirical axial components, determined by fitting the fundamental reflections, predict too much intensity for the satellites, when taken together with spin-only magnitudes of the individual moments. The apparent inconsistency is probably due to the inadequacy of the model; the ferrimagnetic spiral is known to be locally unstable for the particular value of the exchange parameter fixed by the macroscopic moment. Nevertheless, the considerable area of agreement suggests that the conical model is a good first approximation to the ground state.

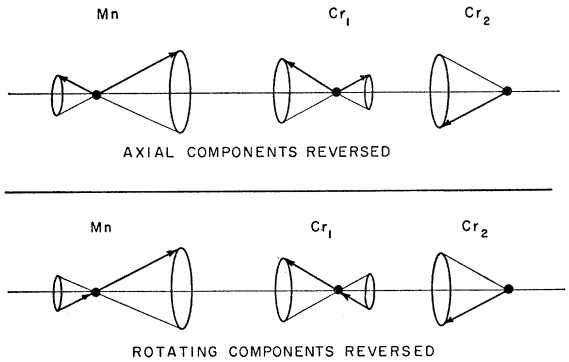

FIG. 10. Schematic representation of two possible models of the magnetic structure of $MnCr_2O_4$ which account for the observed axial and rotating spin components.

It is possible to resolve the apparent discrepancy between the satellite and fundamental intensities, without altering the essential result of the theoretical calculation, provided we introduce a small number (approximately 10%) of reversed spins. The average spin for a given substructure (Mn, Cr_1, Cr_2) instead of lying on a single cone, may, because of the reversed spins, be pictured as belonging to a double cone as shown in Fig. 10. Two limiting possibilities are indicated in the figure: (a) reversed axial components, with transverse components in phase, and (b) axial components in phase, but transverse components reversed.

For the first model, the desired Mn axial moment of 3.68 μ_B can be taken to be the resultant of 4.12 μ_B in the forward direction and 0.44 μ_B in the reverse direction, while the transverse components of 1.83 μ_B and 0.20 μ_B add to give the proper rotating moment. For the Cr_1 sites, an axial component of 1.46 μ_B is obtained by adding 2.06 μ_B in the forward direction and 0.60 μ_B in the reverse direction; the corresponding transverse components, 1.08 μ_B, and 0.31 μ_B, give the desired resultant for the transverse moment. In both instances the cone angles are the theoretical ones and the magnitudes of the moments are the spin-only values. For the Cr_2 sites, the desired axial component of 1.01 μ_B and transverse component of 2.91 μ_B correspond, with no reversed spins, to a total moment of 3.08 μ_B and a cone angle which is only about five degrees greater than that given by theory. Thus, by reversing the axial components of about 10% of the spins, it is possible to obtain approximate agreement with both the satellite and fundamental intensities and at the same time retain a reasonably close fit with the macroscopic moment and the theoretically predicted cone angles, phases, and individual moments. The above scheme is not, however, unique. By reversing the transverse components of some of the spins (model b), similar agreement can be ob-

tained, although in this case the cone angles are no longer close to the theoretical values. The object of the above calculation is to suggest that small perturbations of the ferrimagnetic spiral may well be expected to bring the model into even closer agreement with experiment. A detailed comparison will require not only a further refinement of the theory, but also the collection of more complete experimental data from single crystals.

ACKNOWLEDGMENTS

We are indebted to S. J. Pickart for helpful discussions and for obtaining diffraction data at helium temperatures in the presence of a magnetic field. We wish to thank T. A. Kaplan, K. Dwight, D. A. Lyons, and N. Menyuk for extensive discussion of the theoretical aspects of the ground spin-state problem in spinels.

PHYSICAL REVIEW VOLUME 126, NUMBER 2 APRIL 15, 1962

Theory of Exchange Resonance in Antiferromagnetic $CuCl_2 \cdot 2H_2O$†

R. J. JOENK
Department of Physics, University of Pittsburgh, Pittsburgh, Pennsylvania
(Received December 4, 1961)

The low crystal symmetry of antiferromagnetic $CuCl_2 \cdot 2H_2O$ allows an antisymmetric, anisotropic, superexchange interaction (Moriya interaction) of the form $\mathbf{D}_{12} \cdot [\mathbf{S}_1 \times \mathbf{S}_2]$ between corner and base-center copper ions. The classical magnetic-resonance frequencies and spin-wave frequencies have been derived for a four-sublattice model from a spin Hamiltonian consisting of nearest- and next-nearest-neighbor isotropic superexchange interactions, the Moriya interaction, and orthorhombic anisotropy energy. A set of high-frequency exchange modes was obtained in addition to the usual antiferromagnetic resonance modes. The former are characterized by the beating in opposition of ferromagnetic sublattices which would be degenerate in the absence of the Moriya interaction. The exchange frequencies are proportional to the geometric average of the ferromagnetic and antiferromagnetic exchange fields and are an order of magnitude larger than the antiferromagnetic frequencies. A resonance absorption experiment is proposed to detect the exchange modes; zero field magnetic resonance is expected at about 0.7 mm.

I. INTRODUCTION

IT is well known[1,2] that the presence of anisotropy has a marked effect on the properties of antiferromagnets. Existing theories[3–6] of antiferromagnetic resonance in copper chloride dihydrate have incorporated, in a phenomenological form, the orthorhombic anisotropy energy arising from the anisotropy of the g factor and from the magnetic dipole and pseudodipole interactions. This latter interaction, a combined effect of spin-orbit coupling and exchange interaction, is of second order in the spin-orbit coupling and is symmetric in the interchange of the two spins. Recently Moriya[7] proposed a new mechanism of anisotropic superexchange interaction of the form

$$(\mathcal{H}_m)_{ij} = \mathbf{D}_{ij} \cdot [\mathbf{S}_i \times \mathbf{S}_j], \tag{1}$$

which is linear in the spin-orbit coupling, antisymmetric in the interchange of the two spins, and generally an order of magnitude larger than the pseudodipole coupling. According to Moriya the presence of this interaction in $CuCl_2 \cdot 2H_2O$ results in a canted equilibrium spin configuration.

The effect of the canted spin arrangement in copper chloride is to introduce additional normal modes of vibration in which originally degenerate ferromagnetic sublattices (i.e., degenerate in the absence of the Moriya interaction) beat against each other with a relatively high frequency proportional to the geometric mean of the exchange fields involved. Some of these high-frequency modes exhibit a net magnetization and may be excited by an rf field.

It is the purpose of this paper to derive the magnetic resonance conditions and spin wave dispersion relations for the exchange modes in antiferromagnetic $CuCl_2 \cdot 2H_2O$ and to propose a resonance absorption experiment to detect them. The crystal structure and symmetry elements of $CuCl_2 \cdot 2H_2O$, the spin superstructure, the Moriya interaction, and the four-sublattice model are described in the following section. In Sec. III the resonance frequencies and normal modes of the four-sublattice model are derived from the classical equations of motion at 0°K. An applied field is included in the equations of motion in Sec. IV, and its effect on each of the resonances is discussed. The present theoretical results are compared with experiment and previous

† This work was done in the Sarah Mellon Scaife Radiation Laboratory and was supported by the U. S. Air Force through the Air Force Office of Scientific Research of the Air Research and Development Command.

[1] R. Kubo, Phys. Rev. **87**, 568 (1952).
[2] J. A. Eisele and F. Keffer, Phys. Rev. **96**, 929 (1954).
[3] K. Yosida, Progr. Theoret. Phys. (Kyoto) **7**, 25, 425 (1952).
[4] C. J. Gorter and J. Haantjes, Physica **18**, 285 (1952).
[5] J. Ubbink, Physica **19**, 9 (1953).
[6] T. Nagamiya, Progr. Theoret. Phys. (Kyoto) **11**, 309 (1954).
[7] T. Moriya, Phys. Rev. Letters **4**, 228 (1960); Phys. Rev. **120**, 91 (1960). This theory provides a detailed spin Hamiltonian to account for a macroscopic, phenomenological mechanism proposed by I. Dzialoshinski, J. Phys. Chem. Solids **4**, 241 (1958).